Journal of Nanobiotechnology

RESEARCH

Open Access

NebulaPlate: a droplet microfluidic platform to analyze platelet aggregation

Zheyi Jiang[1†], Meng Wei[1†], Jiawei Zhu[2†], Chenguang Wang[3], Tiantian Zhang[1], Wenjie Zhu[2], Rong Zhang[2], Kandi Zhang[1], Peng Zhang[1], Yihua Lu[1], Alex Chia Yu Chang[1,3*], Yifan Liu[2,4,5*] and Junfeng Zhang[1*]

Abstract

The accurate assessment of platelet activity is crucial in clinical practice and scientific research owing to the pivotal role of platelets in the progression of cardiovascular conditions, such as arterial thrombotic diseases. However, conventional platelet activity assessment methods are currently limited by their requirement of substantial blood samples and inadequate high-throughput capabilities, and therapeutic resistance induced by antiplatelet agents impedes treatment efficacy. In this study, we developed a microdroplet-based platelet function detection method, referred to as NebulaPlate, to achieve miniaturized and robust platelet activity assessment, thereby overcoming current challenges. NebulaPlate supports the merging of platelet samples with drugs confined in picoliter microdroplets and leverages an imaging-based analysis to automatically identify platelets, evaluate their aggregation, and determine P-selectin expression within the anchored microdroplets. We experimentally confirmed the feasibility of aggregation assays on NebulaPlate using various representative antiplatelet drugs. Requiring only 0.3 mL whole blood/chip, which corresponds to approximately 100 platelets/reaction, NebulaPlate reduced the consumption of platelet samples in a single assay. This represents a reduction of 10 times compared to that of conventional techniques. Moreover, our experimental results confirmed the validity and reproducibility of platelet function assays performed using NebulaPlate. Our research highlights important developments in the field of platelet activity assessment and provides fresh prospects for future antiplatelet therapies and personalized medicine. Moreover, it introduces new possibilities for research and clinical practice related to arterial thrombotic diseases.

†Zheyi Jiang, Meng Wei, and Jiawei Zhu equally contributed to this study.

*Correspondence:
Alex Chia Yu Chang
alexchang@shsmu.edu.cn
Yifan Liu
liuyf6@shanghaitech.edu.cn
Junfeng Zhang
jfzhang_dr@163.com

Full list of author information is available at the end of the article

Introduction

Cardiovascular disease (CVD) is the leading cause of death worldwide [1, 2]. From 1990 to 2019, the global prevalence of CVD cases nearly doubled, increasing from 271 million to 523 million [2]. Consequently, the number of CVD-related deaths increased from 12.1 million in 1990 to 18.6 million in 2019 [2]. Projections from the American Heart Association revealed a trend in the future economic burden of CVDs [3]. Among them, ischemic heart disease, which is due to the formation of arterial thrombosis [4], had the highest mortality rate in 2019 of 9.14 million [2]. Platelet activation plays a crucial role in arterial thrombosis development [5–9]. For example,
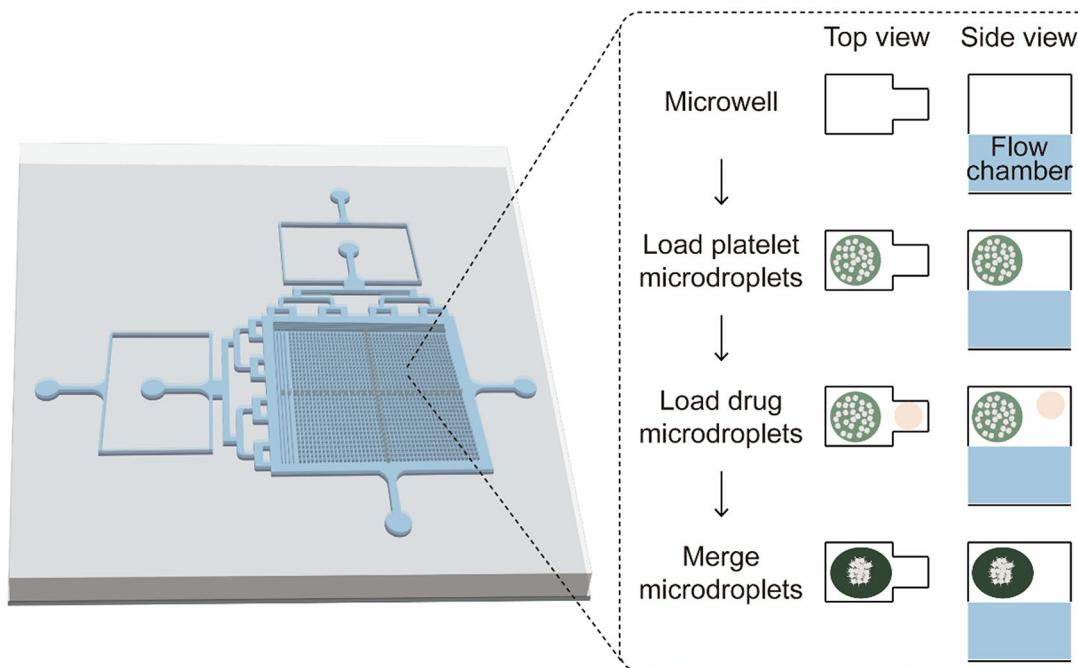
Graphical abstract

when the endothelium of blood vessels becomes damaged or ruptured, the exposed collagen or other platelet agonists, such as thrombin, are bound by specific receptors on the surfaces of platelets. This results in the activation of various signaling pathways that change platelet shape, release granules, and expose phospholipids [8, 10]. These changes enable the adherence and aggregation of platelets to damaged vascular walls and the release of multiple prothrombotic factors, such as adenosine diphosphate (ADP), TXA2, PDGF, and P-selectin (CD62P), thereby amplifying the signal to neighboring platelets [11, 12].

As a critical step in hindering bleeding, platelet aggregation facilitates the accumulation and activation of other clotting factors that transform into stable secondary hemostatic thrombi [8, 12, 13]. Thus, antiplatelet drugs are recognized as the first-line therapy for preventing and treating heart attacks [14, 15]. However, the clinical use of these drugs currently carries significant risks, such as bleeding, gastrointestinal reactions, and drug resistance [16–19]. To assess the risks and treatment options for patients [20–22], understanding the triggers of platelet aggregation and its mechanisms in arterial thrombosis is necessary [8]. Current platelet aggregation detection methods include light transmission aggregometry (LTA), platelet networks, VerifyNow, and whole-blood aggregometry [23]. LTA is currently the gold standard for assessing platelet aggregation [24–26].

In LTA, platelet-rich plasma is activated by a stimulant in the plasma, and the increase in platelet aggregation over time is measured by an increase in light transmission [27, 28]. Because platelet activity can be time-sensitive, large volumes of blood are required for each reaction, and platelet isolation for LTA measurement is labor-intensive [24, 27]. Moreover, individualized anticoagulant regimens are lacking [29–32]. Recently, new products, such as VerifyNow and PFA-200, have been developed to rapidly test platelet function in a small volume of whole blood [33–35]. However, because they use whole blood samples, the complex serum milieu does not offer guidance for personalized anticoagulant decisions [29–32]. Thus, a rapid detection assay that focuses on platelet biology and enables anticoagulant testing is required.

Microfluidic chips are small, highly sensitive, easy to operate after standardization, and inexpensive. They provide an ideal platform for rapid, high-throughput platelet function testing and antiplatelet drug screening. Recently, microfluidic chips have been widely used in biomedical fields, such as DNA sequencing, nucleic acid separation, and quantification, thereby demonstrating its excellent potential in the field of blood analysis [36–39]. Microfluidic devices have been used to simulate in vivo blood flow conditions by mimicking vascular geometries, providing insights into platelet activation sensitivity to different shear stress conditions or drug titration and

clotting time analyses [40–46]. They have also been used to measure the contractile forces generated by platelets during clot formation [47, 48]. However, their designs lack throughput and translatability in clinics. Droplet-based microfluidics may prove an effective solution to this problem. The droplets can be treated as miniature reaction chambers with the potential for utilisation in a diverse array of experiments and applications, including bioanalysis, chemical reactions, and drug screening [49–52]. Additionally, there have been studies conducted on developing a droplet microfluidic strategy for single platelet confinement, with the objective of detecting the function of a single platelet [53, 54]. However, there are no reports on the application of droplet microfluidics for overall platelet function detection.

In this study, we designed a microfluidic chip, referred to as NebulaPlate, to detect platelet aggregation and P-selectin exposure using microdroplet technology. The chip facilitated the loading of a platelet microdroplet and a drug microdroplet into a mixing chamber, and platelet aggregation was observed using microscopy. To establish the robustness of the system, a comparative analysis between NebulaPlate and the gold standard, LTA [24–26] was performed. The rapid and accurate platelet aggregation and P-selectin expression quantification of NebulaPlate facilitated the dose titration evaluation of antiplatelet drugs.

Methods
Additional methods are provided in the supplemental material.

Droplet generation and manipulation
The washed platelets were diluted to 4.26×10^8 or 2.84×10^8 cells/mL for the platelet aggregation or P-selectin tests, respectively, using Tyrode's buffer. The platelets pre-incubated with aspirin, ticagrelor eptifibatide, or prostaglandin I2 (PGI2), and drug solution, including thrombin, ADP, U46619,, or 10 μM Alexa Fluor™ 647 NHS Ester was injected into the droplet generation chip at a flow rate of 400 μL/h using a syringe pump (NE-510, New Era) as the dispersed phase. Moreover, perfluorinated oil (HFE-7500, 3 M) containing 2% (w/w) surfactant (Zhejiang ThunderBio Innovation, Ltd.) was injected at a flow rate of 800 μL/h as the continuous phase. This process required 5 min to complete. The platelet droplets were loaded through the droplet inlet of the NebulaPlate via the negative pressure at the waste liquid outlet. Platelet droplets were first loaded into the large microholes of NebulaPlate at a rate of 50 μL/h based on size selection. Next, the drug droplets were drawn into NebulaPlate and loaded into a small microhole, with a combined process time of 10 min. The fluorinated oil inlets were blocked during droplets loading. Once loaded, the droplet inlets

were closed and the fluorinated oil inlets were opened to flush out unloaded droplets. NebulaPlate was treated with a handheld corona processor (BD-20ACV, Electro-Technic Products) for 5 s to merge the droplets, which were observed under a fluorescence microscope (IX83; Olympus) using 20×/0.8 objective lens (N5702000, Olympus). The fluorophores were excited using a 488 nm laser line (excitation wavelength: 495 nm, emission wavelength: 524 nm, and exposure time: 200 ms) for platelet aggregation or a 640 nm laser line (excitation wavelength: 650 nm, emission wavelength: 660 nm, and exposure time: 240 ms) for P-selectin. Each field of view was continuously recorded for 60–120 min, with images obtained at one-minute intervals. Alternatively, the entire NebulaPlate was only scanned at the beginning and end of the reaction. The microscope settings remained constant to ensure comparability of the results.

Platelet aggregation using NebulaPlate
Platelet aggregation was analyzed using Imaris software (Bitplane, Zurich, Switzerland), which is designed for the visualization, analysis, and interpretation of microscopy datasets. Each analysis required approximately 5 min to complete, and the percentage platelet aggregation was calculated as follows:

$$Aggregation = \frac{initial\ platelet\ area - various\ time\ points\ platelet\ area}{initial\ platelet\ area} \times 100\% \quad (1)$$

Results
Design and fabrication of NebulaPlate
To reduce the volume of blood required for platelet aggregation tests (Fig. 1A), two microfluidic chips were designed for microdroplet generation (Figure S1A and S1B). One reaction chip, NebulaPlate, was designed to facilitate microdroplet loading and microscopic imaging (Figure S1C). Microdroplets containing platelets and drugs with diameters of 80 and 60 μm (Fig. 1B) were generated using a microfluidic chip based on the flow-focusing principle (Figure S1A and S1B) [55–58]. The most stable microdroplets were produced by injecting platelets or drug solutions at a flow rate of 400 μL/h (Figure S3).

NebulaPlate was designed to load and merge microdroplets (Fig. 2A–B and S1C). It comprised an upper layer of 46×32 units facing downward and a lower layer of microdroplet flow chambers (Fig. 1B and S1C). Each unit comprised large and small microwells of widths 69.96 ± 1.30 and 40.04 ± 1.12 μm, respectively (Figure S1C and S2). The microdroplet flow chamber layer with the depth of 80 μm enabled the microdroplets to pass through. Four inlets (two microdroplet and two fluorinated oil inlets) and two outlets were located at the edge of the chip. The microdroplets were loaded through the microdroplet
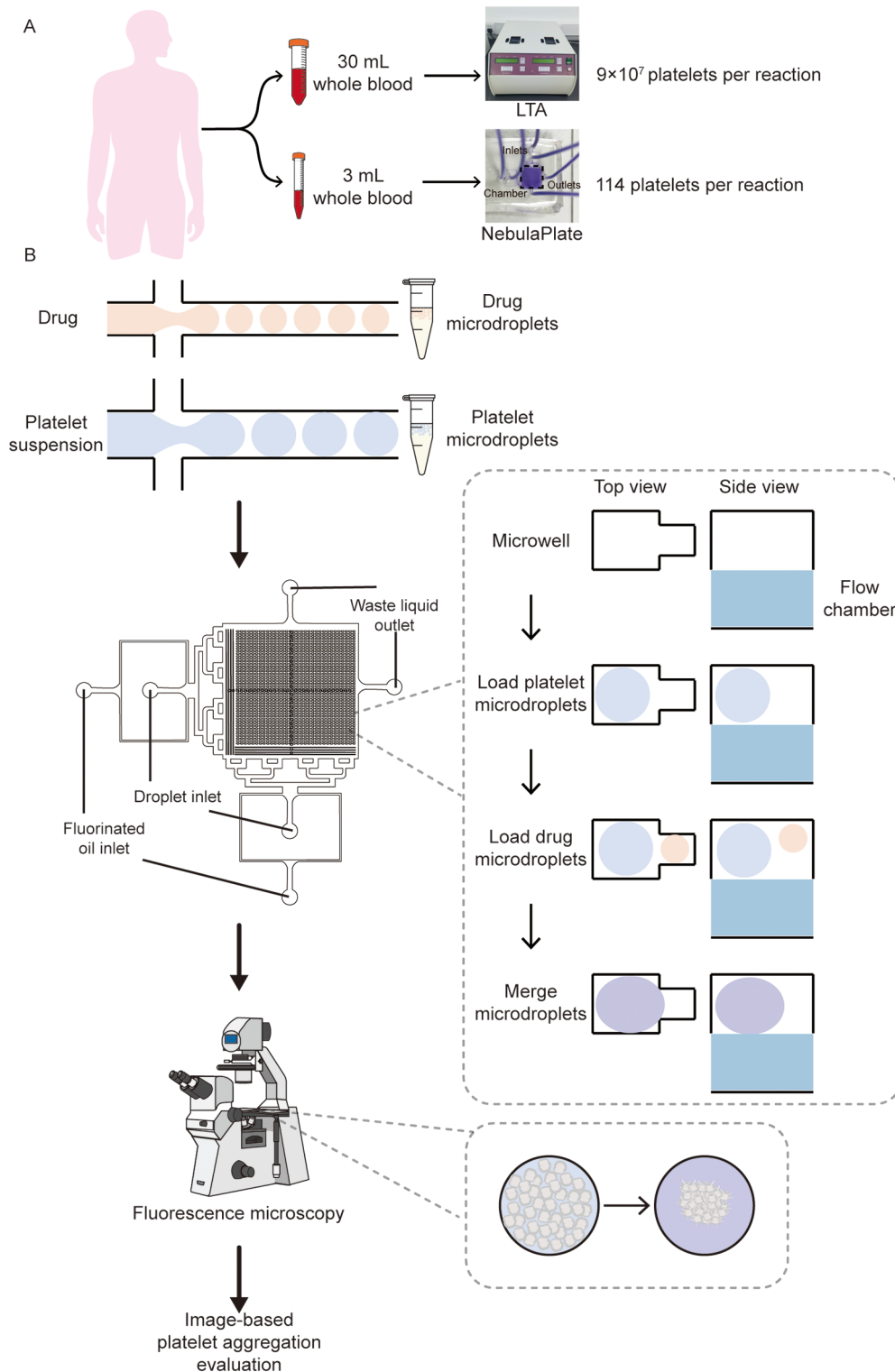
Fig. 1 Design and operation of NebulaPlate. (**A**) Blood requirement using NebulaPlate versus traditional LTA. (**B**) Overview of the NebulaPlate operation

inlet of the NebulaPlate via negative pressure at the waste liquid outlet. Platelet microdroplets were subsequently loaded into large microwells based on the size selection. Drug microdroplets, which included thrombin,

aspirin, and/or ticagrelor, were then drawn into NebulaPlate and loaded into small microwells (Fig. 1B). A corona processor can produce an alternating-current electric field, resulting in interface destabilization and
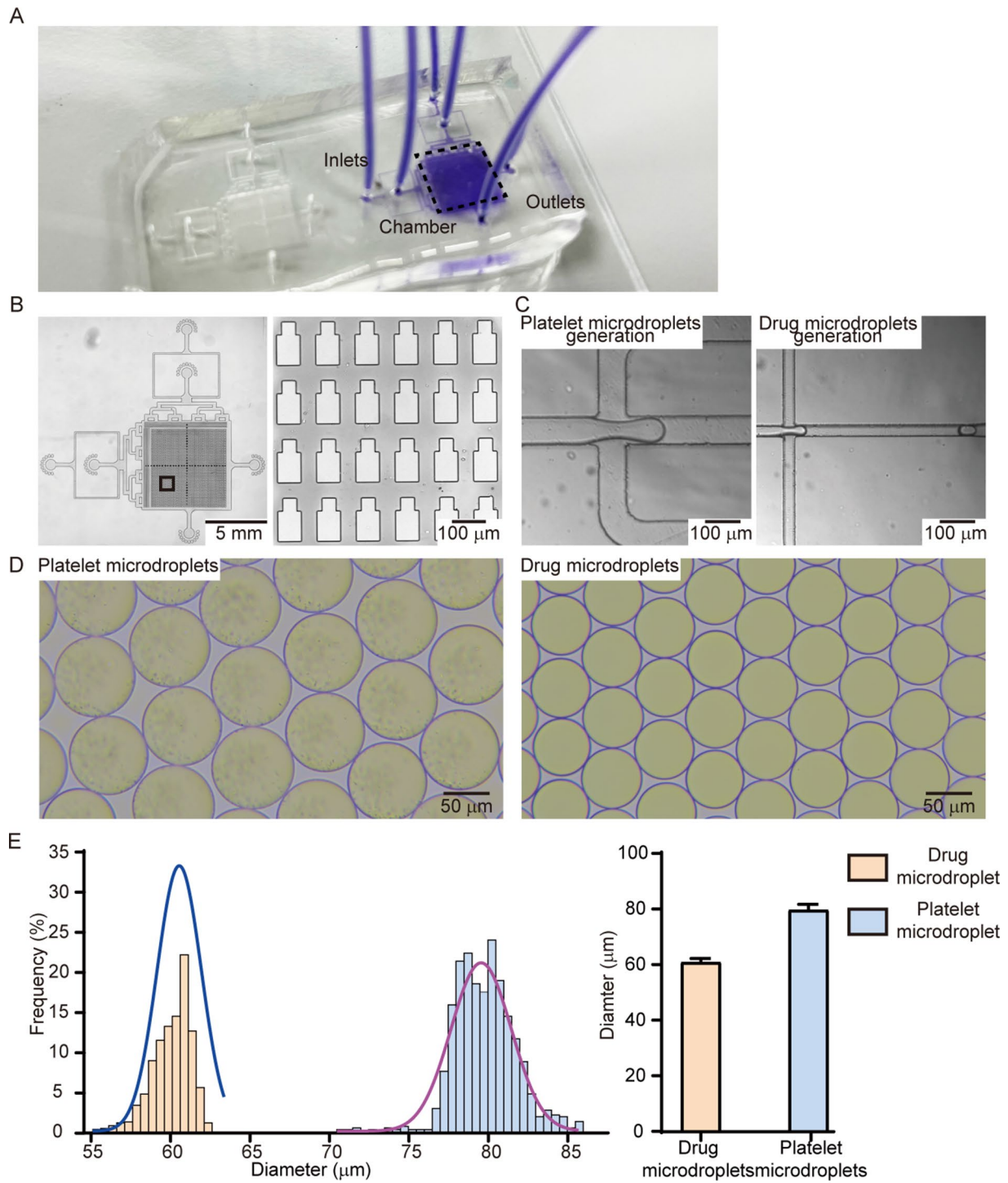
Fig. 2 Standardization of the microdroplet generation. (**A**) Photograph and (**B**) micrograph of the NebulaPlate setup (**C**) Micrograph of the microdroplet generation. (**D**) Representative micrographs of the platelet and drug microdroplets. (**E**) Diameter distribution of the platelet ($n = 989$) and drug ($n = 863$) microdroplets and their average diameters. The data are expressed as mean $\pm$ SD

subsequent microdroplet merging [59]. Thus, an external handheld corona processor was used to electrically fuse the large and small microdroplets. Platelet aggregation was observed using a fluorescence microscope, and the Imaris software was used to identify platelets and calculate their aggregation percentages. The Imaris software is designed for the visualization, analysis, and interpretation of microscopy datasets.

Optimization and standardization of platelet microdroplet generation

Microdroplet uniformity, stability, and resistance to manipulation are crucial factors for consistently measuring platelet aggregation on NebulaPlate. The platelet concentration in the circulation varied in the range of $1–3 \times 10^8$ cells/mL. Because the platelet concentration decreased when the platelet microdroplet fused with the drug microdroplet, $1.42–4.26 \times 10^8$ platelets/mL platelets were encapsulated into the platelet microdroplet to ensure the final platelet concentration in the fused microdroplet remained within a physiological range.

The diameter of the platelet microdroplet was empirically evaluated. A diameter of 80 µm provided the most consistent microdroplet formation efficiency and absence of the spontaneous platelet aggregation (Fig. 2C). The drug microdroplet diameter was set at 60 µm to enable an approximately 3:1 drug dilution when mixed with the platelet microdroplets. A total of 863 small (60.97 ± 1.90 µm diameter average) and 989 large (79.83 ± 1.21 µm diameter average) stable microdroplets were generated, imaged, and quantified (Fig. 2D and E). Theoretically, a merged microdroplet containing 3×10^8/mL platelets should contain approximately 114 platelets (Table 1). The Imaris software for counting indicated that each microdroplet contained an average of 103.2 ± 19.92 platelets (Figure S4), probably because platelets were also distributed in the Z-axis, resulting in a certain loss of platelet data. Owing to the reduction in reaction volume, the agonist consumption per reaction was reduced by three orders of magnitude compared to that of LTA.

We loaded large platelet and small drug microdroplets onto NebulaPlate and calculated the capture rate to determine the efficiency and reliability of microdroplet loading. A total of 8,832 units were analyzed, with 8,111 units (91.84%) correctly loaded with both platelet

Table 1 Platelet utilization efficiency of NebulaPlate and LTA

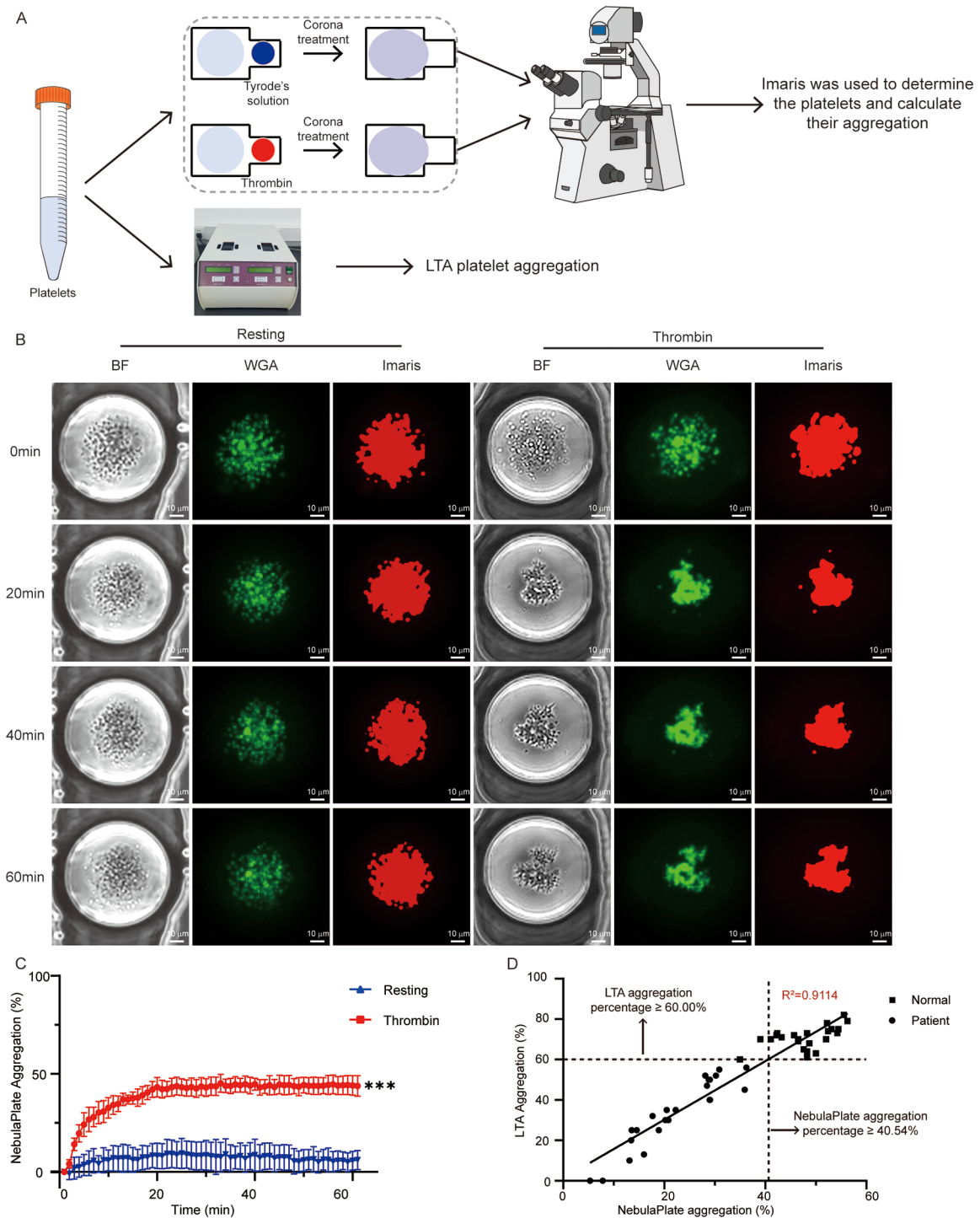|	Theoretical Platelet Count per Reaction System	Minimum Volume of Human Blood Required (mL)
NebulaPlate	114	3 (Available for 10 chips, equals 14720 reactions)
LTA	9×10^7	30 (Available for 12–15 reactions)

and drug microdroplets, 95 units (1.08%) containing only platelet microdroplets, 457 units (5.17%) containing only drug microdroplets, and 169 units (1.91%) without platelet or drug microdroplets (Figure S5). Microdroplet fusion was induced by placing a handheld electrofusion processor, with an induced electric field for 5 s, on top of NebulaPlate. Subsequently, a microdroplet fusion rate of 98.18% (7963 units) was achieved. The uniform distribution of the drug throughout the fused microdroplets following electrofusion was confirmed by adding Alexa Fluor™ 647 NHS Ester to the drug-containing small microdroplets and recording the perfusion of the fluorescence 1 min after electrofusion. We confirmed a uniform distribution of the fluorescent dye in the small fused microdroplets (Figure S6A).

Although cell culture in microdroplets has been well-studied [52], platelet function in microdroplets and the impact of electrofusion on platelet function remain unknown. In this study, platelet aggregation was assayed using the LTA method with a thrombin concentration of 0.75 U/mL (Figure S7A) to ensure the responsiveness of the electrofusion-treated platelets to coagulation induction. No statistical difference was observed for the mean platelet aggregation in the electrofusion-treated (75.50% ± 2.43%) and control (without electrofusion treatment, 78.00% ± 2.10%) groups (Figure S7B). In addition, other standard platelet function assays, including platelet spreading, P-selectin exposure, and clot retraction were performed, which corresponded to activation, propagation, and clot maturation, respectively. The mean platelet spreading area for the electrofusion-treated and control groups were 31.88 ± 1.96 and 32.12 ± 2.39 µm^2, respectively, with no statistical difference (Figure S7C). No difference was observed between the mean P-selectin fluorescence intensities in the resting platelets treated with (219.70 ± 16.10) and without (215.00 ± 18.58) electrofusion (Figure S7D). Moreover, no significant difference was observed between the mean P-selectin fluorescence intensities in the thrombin-challenged platelets treated with (3969.63 ± 116.5 mean fluorescence intensity (MFI)) and without (3839.86 ± 86.66 MFI, Figure S7D) electrofusion. Similarly, the mean clot-retraction ratio showed no statistical difference between the electrofusion-treated (76.80% ± 1.15%) and control (76.97% ± 1.58%) groups (Figure S7E). These results suggested that electrofusion treatment did not affect platelet aggregation.

To detect stable platelet aggregation and standardize the NebulaPlate for robust platelet aggregation evaluation, the optimal thrombin concentration was determined. Thrombin titration experiments were performed, and a concentration of 2 U/mL provided the most stable platelet aggregation (Figure S8A). Platelet aggregation was determined using wheat germ agglutinin (WGA) staining (Fig. 3B). The maximum plateau of

Fig. 3 Accurate platelet aggregation quantification using NebulaPlate. (**A**) Experimental design for confirming the stability of the NebulaPlate. (**B**) Platelet aggregation responses following treatment with distinct drug microdroplets in the NebulaPlate platform, included Tyrode's Buffer (control) and 2 U/mL thrombin (thrombin). (**C**) Temporal evolution of the resting ($n=6$) and 2 U/mL thrombin ($n=6$) platelet aggregation determined as the ratio of the platelet area at different time intervals to the initial platelet area (Formula 1). Platelet aggregation reaches a plateau at 20 min. (**D**) Normal ($n=23$) and patient ($n=23$) platelet aggregation was investigated using both the NebulaPlate and traditional LTA. The data are expressed as mean ± SD, ***$p < 0.001$ vs. resting group

platelet aggregation in NebulaPlate was achieved after 20 min (Fig. 3C), which was longer than that in LTA under stirring (5 min). Thus, LTA was performed without stirring to confirm whether the difference in aggregation time could be attributed to the absence of stirring in the microdroplet system. Consistent with our NebulaPlate observations, the platelets in the unstirred LTA reached maximum aggregation at approximately 20 min (Figure S8B).

Standardization of platelet aggregation on NebulaPlate

We aimed to standardize the quantification of time-lapse videos captured using NebulaPlate. Platelet aggregation was quantified using commercial Imaris segmentation. Activated platelets in the blood adhered to damaged vessel walls and released secondary signals such as ADP to attract more platelets, resulting in aggregation [8, 13]. Similarly, the platelets in our microdroplets were activated and gradually aggregated with other platelets to form clusters, whereas the number of free platelets decreased over time (Supplementary Movie 1). Therefore, the ratio of platelet area at various time points to the initial platelet area could serve as a quantitative measure of platelet aggregation (Formula 1).

Platelet recognition was enhanced using the live-cell WGA stain conjugated with Alexa Fluor 488, followed by segmentation in Imaris (Fig. 3A). The Imaris software successfully identified platelets (Fig. 3B), enabling the time-dependent determination of platelet aggregation (Fig. 3C and S9A-B). The reliability of NebulaPlate was assessed and compared with that of LTA (Fig. 3D). Platelets were isolated from 46 individuals, including 23 healthy volunteers and 23 cardiovascular patients on antiplatelet drug medications, and platelet aggregation was evaluated using both NebulaPlate and LTA. In the 23 healthy samples, platelet aggregation attained $\geq 60\%$ using LTA, whereas 21 of them exhibited platelet aggregation $\geq 40.54\%$ using NebulaPlate. For the 23 cardiovascular patients, platelet aggregation was $< 60\%$ using LTA, whereas 23 of the samples exhibited an aggregation of $< 40.54\%$ using NebulaPlate. Using the best-fit line, platelet aggregation between the two systems correlated well, with $R^2 = 0.9114$. These results demonstrated the robustness of the NebulaPlate system in measuring platelet aggregation.

Validation of the performance of NebulaPlate with common antiplatelet drugs

The sensitivity of NebulaPlate to antiplatelet drugs was confirmed using clinically prescribed aspirin and ticagrelor. Platelet aggregation was used to evaluate and compare NebulaPlate and conventional LTA. First, untreated normal platelets were encapsulated in microdroplets, and Imaris was used for automated platelet recognition and

analysis to obtain a baseline platelet aggregation profile. Subsequently, the platelets pre-incubated with aspirin (50, 100, and 200 µM) or ticagrelor (10, 30, and 50 µM) were separately encapsulated in microdroplets and analyzed using Imaris (Fig. 4A). The platelet aggregation percentages following treatment with 0, 50, 100, and 200 µM aspirin were 52.62% ± 7.82%, 36.64% ± 5.54%, 18.33% ± 5.87%, and 5.82 ± 2.07%, respectively, for NebulaPlate (Fig. 4B) and 74.33% ± 4.13%, 68.00% ± 8.46%, 69.17% ± 8.93%, and 67.17% ± 8.84%, respectively, for LTA (Fig. 4C). The platelet aggregation percentages following treatment with 0, 10, 30, and 50 µM ticagrelor were 51.74% ± 6.93%, 22.06% ± 4.33%, 14.92% ± 3.27%, and 3.90% ± 1.99%, respectively, for NebulaPlate (Fig. 4D) and 70.83% ± 7.36%, 44.17% ± 9.70%, 24.17% ± 5.85%, and 5.17% ± 2.56%, respectively, for LTA (Fig. 4E). The aggregation results using NebulaPlate displayed good sensitivity to the antiplatelet drug concentration, with good reproducibility (Fig. 4B–E and S9C). Furthermore, fluorescently labelled droplets of varying drugs were loaded into the same NebulaPlate, and the platelet aggregation percentage were subsequently measured (Figure S10A). The results demonstrated that the platelet aggregation rate was 5.89% ± 4.25% in the resting group, 55.59% ± 12.94% in the thrombin group, 16.58% ± 9.40% in the aspirin group, and 14.70% ± 8.20% in the ticagrelor group (Figure S10B). These data supported the robustness of NebulaPlate for mid- to high-throughput platelet aggregation testing. Overall, NebulaPlate and Imaris exhibited good performance in detecting platelet aggregation, with good reliability and practicality. In particular, NebulaPlate could significantly reduce the number of platelets required and improve detection efficiency. It could be widely applicable in different fields, including clinical antiplatelet drug screening and therapeutic effect evaluation.

### P-selectin membrane localization analysis using NebulaPlate

Considering the significant advantages of NebulaPlate for visualization, its ability to detect P-selectin membrane expression in activated platelets was investigated. APC-conjugated CD62P (P-selectin) fluorescent antibodies were co-encapsulated in drug microdroplets, and the membrane P-selectin expression in platelets was monitored following electrofusion (Fig. 5A). The microdroplets containing thrombin or Tyrode's buffer (Fig. 5B) were separately analyzed. Over time, P-selectin expression in activated platelets gradually increased and attained a stable level after 40 min. Conversely, the resting platelets exhibited no significant changes. Furthermore, there was a gradual increase in P-selectin expression with increases in thrombin concentration (Fig. 5C). The platelets were subsequently treated with a clinically relevant antiplatelet
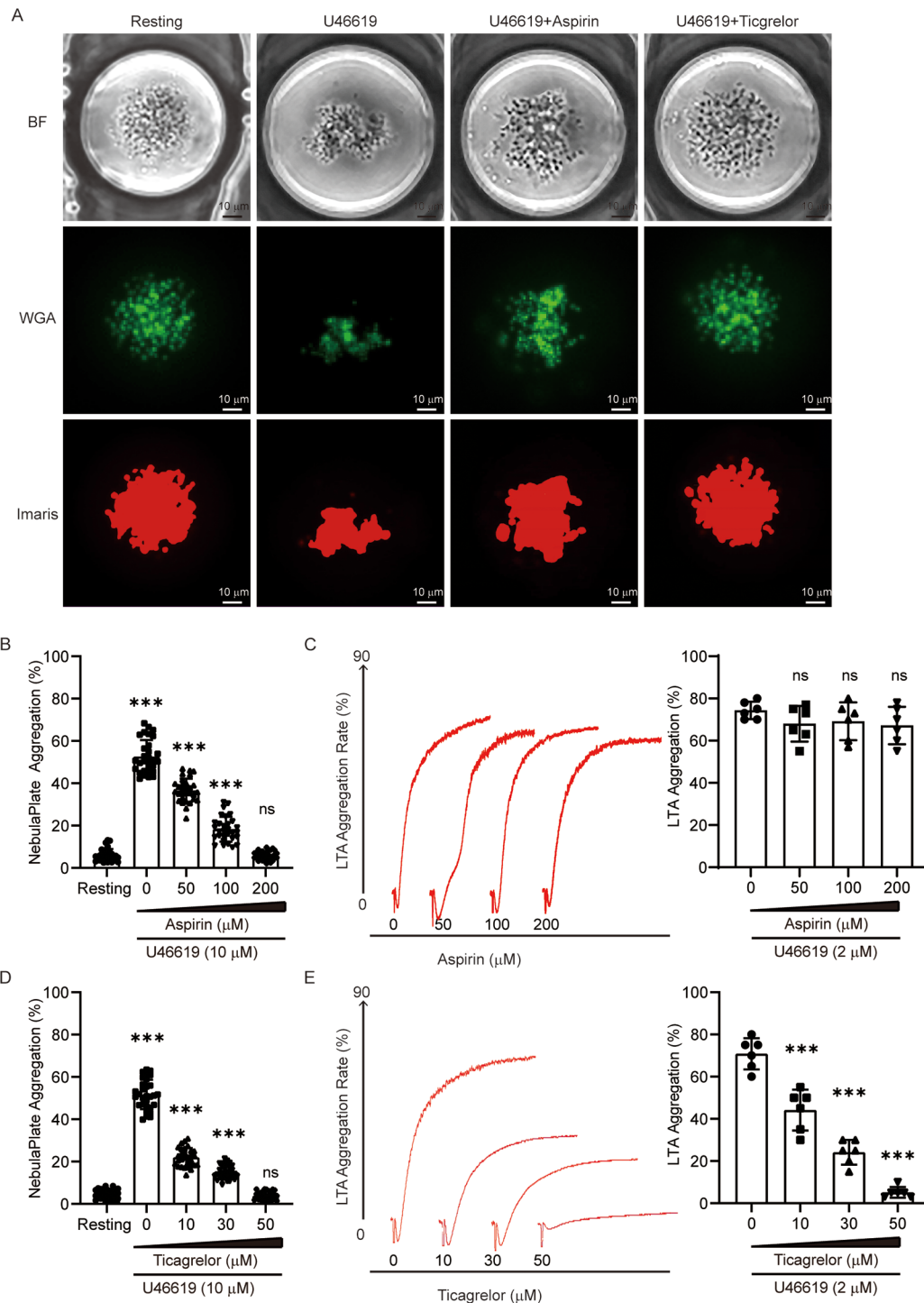
Fig. 4 Validation of NebulaPlate stability with different antiplatelet drug treatments. **A**. Platelet aggregation responses of different drug-treated platelets within the NebulaPlate platform at 20 min (U46619: 10 U/mL; aspirin: 100 μM; ticagrelor: 30 μM). **B**, **D**. Platelet aggregation under varying concentrations of aspirin or ticagrelor assessed using the NebulaPlate platform (*n* = 30). **C**, **E**. Platelet aggregation under varying concentrations of aspirin or ticagrelor, measured using LTA (*n* = 6). The data are expressed as mean ± SD, *$p < 0.05$, **$p < 0.01$, and ***$p < 0.001$ vs. resting or 0 group

drug, aspirin, and their P-selectin expression on the NebulaPlate was analyzed to further confirm the results. The platelets were subjected to 100 and 200 μM aspirin while the P-selectin expression levels were monitored following

thrombin stimulation (Figure S11). The fluorescence intensity of P-selectin corresponded to the results of platelet aggregation. The relative fluorescence intensities for the resting, thrombin, 100 μM aspirin, and 200 μM

Jiang *et al. Journal of Nanobiotechnology* (2025) 23:171

Page 10 of 14
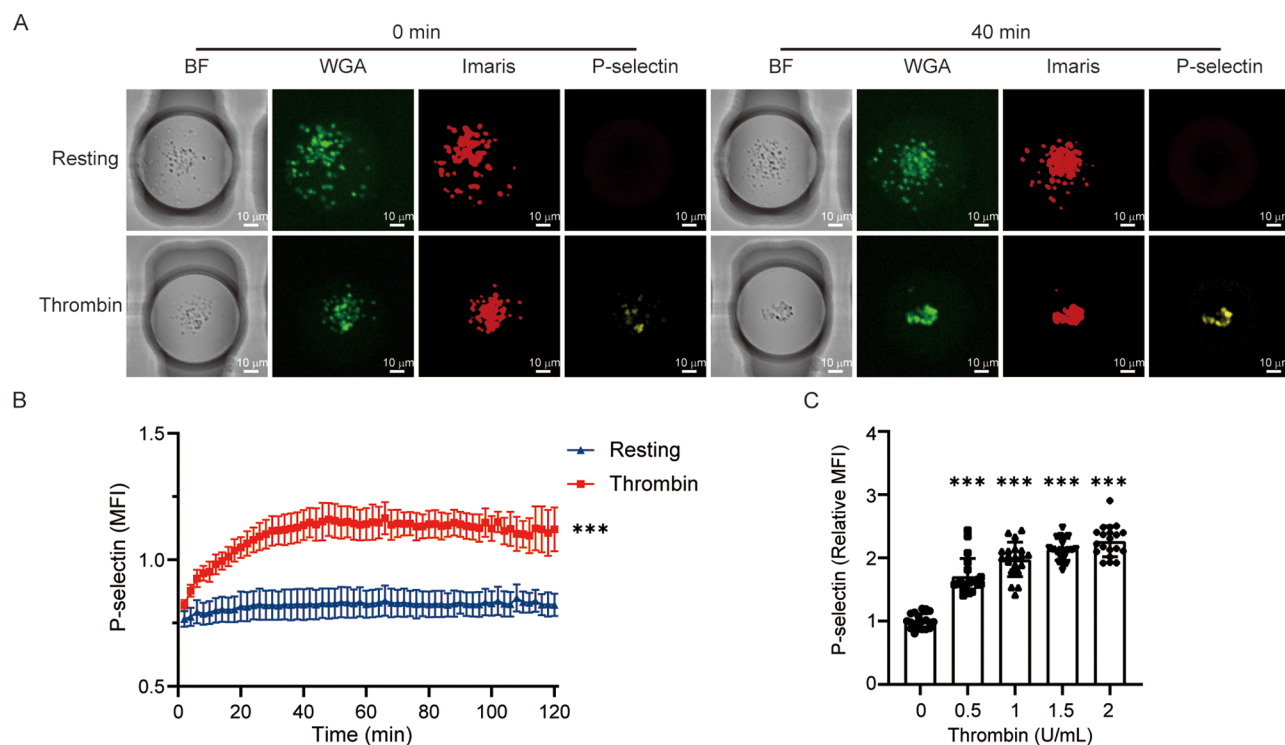
Fig. 5 P-selectin exposure in NebulaPlate. (**A**) Platelet P-selectin exposure responses following treatment with different drug microdroplets in the NebulaPlate platform with Tyrode's buffer (resting) or 2 U/mL thrombin (thrombin). Platelet concentration: 2×10^8 /mL. (**B**) Temporal evolution of the resting ($n=6$) and 2 U/mL thrombin ($n=6$) platelet P-selectin exposure. P-selectin expression reaches a plateau at 40 min. (**C**) Platelet P-selectin exposure treated with Tyrode's buffer or different concentrations of thrombin ($n=20$) at 40 min. The data are expressed as mean ± SD, ***$p < 0.001$ vs. 0 group

aspirin groups were 1.00 ± 0.09, 2.12 ± 0.40, 1.42 ± 0.14, and 0.96 ± 0.08, respectively. The platelet aggregations of the resting, thrombin, 100 μM aspirin, and 200 μM aspirin groups were 4.97 ± 1.56, 44.69 ± 6.49, 20.23 ± 4.66, and 4.61 ± 1.59, respectively. These findings demonstrated that NebulaPlate could be used to assess platelet functionality by measuring P-selectin expression.

Discussion

In this study, we designed and validated a microfluidic droplet-based platelet aggregation system, NebulaPlate, which enabled the efficient, sensitive, and low-cost evaluation of platelet aggregation and P-selectin exposure. Although LTA, which measures the percentage of platelet aggregation via light transmission, is the gold standard for detecting platelet aggregation [24–26], it requires numerous platelets (9×10^7 /reaction or 20–30 mL of fresh blood) and at least six technical replicates to confirm measurements. In contrast, the proposed NebulaPlate platform requires only 2–3 mL of whole blood to generate over 15,000 microdroplets (sufficient for 10 chips). In theory, one LTA test affords 789,473 reactions on NebulaPlate (Table 1), demonstrating its potential for personalized antiplatelet prescriptions and mid- to high-throughput antiplatelet drug discovery. We also demonstrated that platelet microdroplets could be electrically

fused with drug microdroplets and that platelet aggregation and P-selectin surface expression could be monitored over time.

NebulaPlate required a small number of platelets, with each microdroplet containing approximately 114 platelets. Considering their lifespan [60], heterogeneous properties of platelet function may exist when only a small number of platelets are tested. However, the standard deviations of the results obtained with NebulaPlate were lower than those obtained with LTA (Fig. 4). Furthermore, the number of technical reactions was considerably higher owing to the miniaturization of NebulaPlate, which improved the reliability of the results.

NebulaPlate required a considerably higher agonists concentration and longer reaction time than the LTA system for several reasons. First, the standard LTA method involves stirring during platelet aggregation, thereby increasing the shear force while enhancing platelet activation [61]. Second, despite matching the platelet concentration to that used in LTA, the reaction microdroplets contained fewer platelets in NebulaPlate, which could limit platelet aggregation driven by positive feedback signaling [62]. This was supported by the results reported by Jongen et al. [54], in which the activation thresholds for single platelets were higher than those for collective platelets. Third, the system required 10 min to

set up the actual aggregated data collection, which lasted for 30 min. This period ensured a high accuracy of the captured platelet activity [27].

The role of shear force in platelet activation has been extensively investigated [61]. Numerous previous studies have increased the shear force by simulating the microvasculature using microfluidics [44–46], thereby more closely matching the physiological or pathological environment in vivo. However, we did not incorporate shear forces into our system because using a fixed shear force to assess platelet activation does not recapitulate physiological variables such as vascular diameter, blood pressure, and vessel curvature. Thus, false negatives for potential antiplatelet drugs could be obtained using the LTA assay because shear force was applied owing to the aggregation chain reaction initiated by more platelets undergoing non-physiological shear stress. Several microfluidic chips designed for platelet function have adopted a pipette-based design that facilitates control of the shear force by adjusting the flow rate, channel shape, and diameter [63]. However, these designs inevitably expose platelets to the channel walls, increasing concerns about the impact of channel material on platelet function [47]. Thus, the encapsulation of platelets within microdroplets eliminates these concerns. Nevertheless, given the significance of shear on platelet function, it is possible that future methodologies may facilitate more effective incorporation of shear within microdroplets, thereby enhancing the ability to replicate in vivo microenvironments.

In our NebulaPlate system, the platelet aggregation function was assessed without considering fluid mechanics. As expected, platelet aggregation was positively correlated with stimulus concentration (Figure S8A). For example, a higher aggregation stimulus resulted in faster platelet aggregation.

In high-throughput platelet function testing, well-plate-based aggregation assays have been widely adopted as alternative methods for assessing platelet function in high-throughput environments [64, 65]. Despite the extensive utilization of 96-well or 384-well microplates in high-throughput screening, their fixed observational dimensions limits any further upgrade in terms of throughput. In the context of microdroplets, the amount of sample required is significantly diminished given the small volume and foreseeably optimized optics with automation can allow further upgrade in throughput and drug randomization if one uses fluorescence barcoding.

As a cell-surface glycoprotein, P-selectin plays a pivotal role in activating and amplifying aggregation signals [7, 66, 67]. In response to vascular damage, platelets release granules containing P-selectin to induce platelet adhesion to endothelial cells and initiate thrombus formation [68]. In addition, P-selectin serves as an inflammatory signal by promoting leukocyte migration and adhesion, thereby propagating the inflammatory response [69, 70]. Because NebulaPlate enabled the visualization of P-selectin levels during platelet aggregation, this microdroplet reaction chamber offers a new platform for examining platelet activation. We found that the expression of P-selectin gradually increased with the increase of thrombin concentration (Fig. 5C). However, the rate of increase was observed to gradually decelerate. This indicates the potential for P-selectin sites to be covered by platelets following aggregation. Nevertheless, this hypothesis requires further investigation.

U46619 is an agonist of the platelet thromboxane receptors, which is not generally considered to be targeted by aspirin. It is well known that aspirin exerts its effect by impeding the synthesis of thromboxane within platelets. It has been suggested that in presence of exogenous thromboxane, efficacy of aspirin to block intracellular thromboxane synthesis is diminished [71]. However, our experimental data presented in Fig. 4 appear to contradict this hypothesis, thereby suggesting that the NebulaPlate platform may exhibit an excessive reliance on *de novo* thromboxane production (more sensitive to U46619). This phenomenon may be particularly pronounced in low-calcium environments, where platelets exhibit heightened sensitivity to certain aggregating agents [72]. Consequently, subsequent enhancements to the NebulaPlate platform are imperative.

Conclusion

NebulaPlate exhibits various features and advantages that may be of interest to the cardiovascular community. First, it uses a small volume of blood to reduce sample consumption and cost. Second, it integrates standard markers for assessing platelet function and uses microfluidic droplet technology to facilitate platelet aggregation studies without shear stress complications. Third, dose titration and combinatorial prescriptions can be easily personalized using a standalone platelet aggregation device with built-in optics and column partitioning of preestablished antiplatelet drugs at varying dosages. Finally, the data processing of NebulaPlate is sufficiently robust for commercial and noncommercial software, which can be further streamlined to improve efficiency.

We also acknowledge certain limitations with our study. For example, NebulaPlate requires 2–3 mL of whole blood because platelet isolation is not currently incorporated into its microfluidic chip design. Moreover, the current camera settings only enable the simultaneous recording of 18 microdroplets. We envision that this problem can be overcome by designing a smaller chip/parallel microscopy setup for live-cell tracking. The current time-consuming data analysis procedure negates the advantage of high throughput. This may be accomplished

Jiang *et al. Journal of Nanobiotechnology*　　　(2025) 23:171

Page 12 of 14

by optimizing the algorithms to facilitate a more efficient process.

Abbreviations

ADP　　　Adenosine diphosphate
CVD　　　Cardiovascular disease
LTA　　　Light transmission aggregometry
WGA　　　Wheat germ agglutinin
PGI2　　　Prostaglandin I2

Supplementary Information

The online version contains supplementary material available at https://doi.org/10.1186/s12951-025-03212-5.

Supplementary Material 1

Data availability

No datasets were generated or analysed during the current study.

Declarations

Ethics approval and consent to participate

This study was conducted in accordance with the Declaration of Helsinki and was approved by the Shanghai Ninth People's Hospital, Shanghai Jiao Tong University School of Medicine Ethics Committee, and informed consent was obtained from all the participants.

Consent for publication

All authors agreed to publish this manuscript.

Competing interests

The authors declare no competing interests.

Author details

[1]Department of Cardiology, Shanghai Ninth People's Hospital, Shanghai Jiao Tong University School of Medicine, Shanghai 200011, China
[2]School of Physical Science and Technology, ShanghaiTech University, Shanghai 201210, China
[3]Shanghai Institute of Precision Medicine, Ninth People's Hospital, Shanghai Jiao Tong University School of Medicine, Shanghai 200125, China
[4]Shanghai Clinical Research and Trial Center, Shanghai 201210, China
[5]State Key Laboratory of Advanced Medical Materials and Devices, ShanghaiTech University, Shanghai 201210, China

References

1. Sacco RL, Roth GA, Reddy KS, Arnett DK, Bonita R, Gaziano TA, et al. The heart of 25 by 25: achieving the goal of reducing global and regional premature deaths from cardiovascular diseases and stroke: a modeling study from the American heart association and world heart federation. Circulation. 2016;133:e23674–90. https://doi.org/10.1161/CIR.0000000000000395. Epub 20160509.
2. Roth GA, Mensah GA, Johnson CO, Addolorato G, Ammirati E, Baddour LM, et al. Global burden of cardiovascular diseases and risk factors, 1990–2019: update from the gbd 2019 study. J Am Coll Cardiol. 2020;76:25:2982–3021. https://doi.org/10.1016/j.jacc.2020.11.010.
3. Dunbar SB, Khavjou OA, Bakas T, Hunt G, Kirch RA, Leib AR, et al. Projected costs of informal caregiving for cardiovascular disease: 2015 to 2035: a policy statement from the American heart association. Circulation. 2018;137:e19558–77. https://doi.org/10.1161/CIR.0000000000000570. Epub 20180409.
4. Davies MJ, Thomas A. Thrombosis and acute coronary-artery lesions in sudden cardiac ischemic death. N Engl J Med. 1984;310:18:1137–40. https://doi.org/10.1056/NEJM198405033101801.
5. Koupenova M, Clancy L, Corkrey HA, Freedman JE. Circulating platelets as mediators of immunity, inflammation, and thrombosis. Circ Res. 2018;122(2):337–51. https://doi.org/10.1161/CIRCRESAHA.117.310795.
6. Davi G, Patrono C. Platelet activation and atherothrombosis. N Engl J Med. 2007;357:24. https://doi.org/10.1056/NEJMra071014. Epub 2007/12/14.
7. Furie B, Furie BC. Role of platelet p-selectin and microparticle psgl-1 in thrombus formation. Trends Mol Med. 2004;10(4):171–8. https://doi.org/10.1016/j.molmed.2004.02.008.
8. van der Meijden PEJ, Heemskerk JWM. Platelet biology and functions: new concepts and clinical perspectives. Nat Rev Cardiol. 2019;16(3):166–79. https://doi.org/10.1038/s41569-018-0110-0.
9. Estevez B, Du X. New concepts and mechanisms of platelet activation signaling. Physiol (Bethesda). 2017;32(2):162–77. https://doi.org/10.1152/physiol.00020.2016.
10. Weber C. Platelets and chemokines in atherosclerosis: partners in crime. Circ Res. 2005;96:6:612–6. https://doi.org/10.1161/01.RES.0000160077.17427.57.
11. Xu XR, Carrim N, Neves MA, McKeown T, Stratton TW, Coelho RM et al. Platelets and platelet adhesion molecules: Novel mechanisms of thrombosis and anti-thrombotic therapies. Thromb J. 2016;14:Suppl 1:29. Epub 20161004 https://doi.org/10.1186/s12959-016-0100-6
12. Huang J, Li X, Shi X, Zhu M, Wang J, Huang S, et al. Platelet integrin alphaiibbeta3: Signal transduction, regulation, and its therapeutic targeting. J Hematol Oncol. 2019;12(1):26. https://doi.org/10.1186/s13045-019-0709-6. Epub 20190307.
13. Jackson SP. The growing complexity of platelet aggregation. Blood. 2007;109:12. Epub 20070220 doi: 10.1182/blood-2006-12-027698.
14. Lawton JS, Tamis-Holland JE, Bangalore S, Bates ER, Beckie TM, Bischoff JM, et al. 2021 acc/aha/scai guideline for coronary artery revascularization: a report of the American college of cardiology/american heart association joint committee on clinical practice guidelines. J Am Coll Cardiol. 2022;79:e221–129. https://doi.org/10.1016/j.jacc.2021.09.006. Epub 20211209.
15. Alexopoulos D, Xanthopoulou I, Deftereos S, Hamilos M, Sitafidis G, Kanakakis I, et al. Contemporary antiplatelet treatment in acute coronary syndrome patients undergoing percutaneous coronary intervention: 1-year outcomes from the Greek antiplatelet (grape) registry. J Thromb Haemost. 2016;14:6. https://doi.org/10.1111/jth.13316. Epub 20160504.
16. Bittl JA, Laine L. Gastrointestinal injury caused by aspirin or clopidogrel monotherapy versus dual antiplatelet therapy. J Am Coll Cardiol. 2022;79:2:129– 31. Epub 20211106 https://doi.org/10.1016/j.jacc.2021.10.027
17. Kalyanasundaram A, Lincoff AM, Medscape. Managing adverse effects and drug-drug interactions of antiplatelet agents. Nat Rev Cardiol. 2011;8:10:592–600. https://doi.org/10.1038/nrcardio.2011.128. Epub 20110913.
18. Sweeny JM, Gorog DA, Fuster V. Antiplatelet drug 'resistance'. Part 1: mechanisms and clinical measurements. Nat Rev Cardiol. 2009;6(4):273–82. https://doi.org/10.1038/nrcardio.2009.10.
19. Kuliczkowski W, Witkowski A, Polonski L, Watala C, Filipiak K, Budaj A et al. Interindividual variability in the response to oral antiplatelet drugs: A position paper of the working group on antiplatelet drugs resistance appointed by

the section of cardiovascular interventions of the polish cardiac society, endorsed by the working group on thrombosis of the european society of cardiology. Eur Heart J. 2009;30:4:426–35. Epub 20090127 https://doi.org/10.1093/eurheartj/ehn562

20. Hally KE, Parker OM, Brunton-O'Sullivan MM, Harding SA, Larsen PD. Linking neutrophil extracellular traps and platelet activation: a composite biomarker score for predicting outcomes after acute myocardial infarction. Thromb Haemost. 2021;121:12. https://doi.org/10.1055/s-0041-1728763. Epub 20210513.

21. Adatia K, Farag MF, Gue YX, Srinivasan M, Gorog DA. Relationship of platelet reactivity and inflammatory markers to recurrent adverse events in patients with St-elevation myocardial infarction. Thromb Haemost. 2019;119:11. https://doi.org/10.1055/s-0039-1695007. Epub 20190822.

22. Chu SG, Becker RC, Berger PB, Bhatt DL, Eikelboom JW, Konkle B et al. Mean platelet volume as a predictor of cardiovascular risk: A systematic review and meta-analysis. J Thromb Haemost. 2010;8:1:148–56. Epub 20090819 https://doi.org/10.1111/j.1538-7836.2009.03584.x

23. Lordkipanidze M. Platelet function tests. Semin Thromb Hemost. 2016;42:3:258–67. Epub 20160229 doi: 10.1055/s-0035-1564834.

24. Le Blanc J, Mullier F, Vayne C, Lordkipanidze M. Advances in platelet function testing-light transmission aggregometry and beyond. J Clin Med. 2020;9:8. https://doi.org/10.3390/jcm9082636. Epub 20200813.

25. Althaus K, Zieger B, Bakchoul T, Jurk K, Hamatologie, TH-PSdGfT-uHudGfPOu. Standardization of light transmission aggregometry for diagnosis of platelet disorders: an inter-laboratory external quality assessment. Thromb Haemost. 2019;119:7. https://doi.org/10.1055/s-0039-1688791. Epub 20190602.

26. Born GV. Aggregation of blood platelets by adenosine diphosphate and its reversal. Nature. 1962;194:927–9. https://doi.org/10.1038/194927b0.

27. Gomez K, Anderson J, Baker P, Biss T, Jennings I, Lowe G, et al. Clinical and laboratory diagnosis of heritable platelet disorders in adults and children: a British society for haematology guideline. Br J Haematol. 2021;195:1. https://doi.org/10.1111/bjh.17690. Epub 20210826.

28. Cattaneo M, Cerletti C, Harrison P, Hayward CP, Kenny D, Nugent D, et al. Recommendations for the standardization of light transmission aggregometry: a consensus of the working party from the platelet physiology subcommittee of ssc/isth. J Thromb Haemost. 2013. https://doi.org/10.1111/jth.12231. Epub 20130410.

29. Cayla G, Cuisset T, Silvain J, Leclercq F, Manzo-Silberman S, Saint-Etienne C, et al. Platelet function monitoring to adjust antiplatelet therapy in elderly patients stented for an acute coronary syndrome (antarctic): an open-label, blinded-endpoint, randomised controlled superiority trial. Lancet. 2016;388:100552015–22. https://doi.org/10.1016/S0140-6736(16)31323-X. Epub 20160828.

30. Trenk D, Stone GW, Gawaz M, Kastrati A, Angiolillo DJ, Muller U, et al. A randomized trial of prasugrel versus clopidogrel in patients with high platelet reactivity on clopidogrel after elective percutaneous coronary intervention with implantation of drug-eluting stents: results of the trigger-pci (testing platelet reactivity in patients undergoing elective stent placement on clopidogrel to guide alternative therapy with prasugrel) study. J Am Coll Cardiol. 2012;59:24. https://doi.org/10.1016/j.jacc.2012.02.026. Epub 20120418.

31. Price MJ, Angiolillo DJ, Teirstein PS, Lillie E, Manoukian SV, Berger PB, et al. Platelet reactivity and cardiovascular outcomes after percutaneous coronary intervention: a time-dependent analysis of the gauging responsiveness with a verifynow p2y12 assay: impact on thrombosis and safety (gravitas) trial. Circulation. 2011;124:101132–7. https://doi.org/10.1161/CIRCULATIONAHA.111.029165. Epub 20110829.

32. Collet JP, Cayla G, Cuisset T, Elhadad S, Range G, Vicaut E et al. Randomized comparison of platelet function monitoring to adjust antiplatelet therapy versus standard of care: Rationale and design of the assessment with a double randomization of (1) a fixed dose versus a monitoring-guided dose of aspirin and clopidogrel after des implantation, and (2) treatment interruption versus continuation, 1 year after stenting (arctic) study. Am Heart J. 2011;161:1:5–12 e5 https://doi.org/10.1016/j.ahj.2010.09.029

33. Favaloro EJ, Pasalic L, Lippi G. Towards 50 years of platelet function analyser (pfa) testing. Clin Chem Lab Med. 2023;61:5:851–60. Epub 20220721 https://doi.org/10.1515/cclm-2022-0666

34. Park SJ, Yoon J, Seo HS, Lim CS. Performance evaluation of the anysis-200 platelet function analyzer in cardiac patients. Clin Hemorheol Microcirc. 2022;80(1):17–24. https://doi.org/10.3233/CH-190801.

35. Marcucci R, Gori AM, Paniccia R, Giusti B, Valente S, Giglioli C, et al. Cardiovascular death and nonfatal myocardial infarction in acute coronary syndrome patients receiving coronary stenting are predicted by residual platelet reactivity to adp detected by a point-of-care assay: a 12-month follow-up.

Circulation. 2009;119:2237–42. https://doi.org/10.1161/CIRCULATIONAHA.108.812636. Epub 20081231.

36. Battat S, Weitz DA, Whitesides GM. An outlook on microfluidics: The promise and the challenge. Lab Chip. 2022;22:3:530-6. Epub 20220201 https://doi.org/10.1039/d1lc00731a

37. Shang L, Cheng Y, Zhao Y. Emerging droplet microfluidics. Chem Rev. 2017;117:12:7964–8040. https://doi.org/10.1021/acs.chemrev.6b00848.

38. Sackmann EK, Fulton AL, Beebe DJ. The present and future role of microfluidics in biomedical research. Nature. 2014;507:7491:181–9. https://doi.org/10.1038/nature13118.

39. Tan SY, Leung Z, Wu AR. Recreating physiological environments in vitro: Design rules for microfluidic-based vascularized tissue constructs. Small. 2020;16:9:e1905055. Epub 20200108 https://doi.org/10.1002/smll.201905055

40. Santos-Martinez MJ, Prina-Mello A, Medina C, Radomski MW. Analysis of platelet function: role of microfluidics and nanodevices. Analyst. 2011;136:24:5120–6. https://doi.org/10.1039/c1an15445a. Epub 20111026.

41. Tovar-Lopez FJ, Rosengarten G, Westein E, Khoshmanesh K, Jackson SP, Mitchell A, et al. A microfluidics device to monitor platelet aggregation dynamics in response to strain rate micro-gradients in flowing blood. Lab Chip. 2010;10:3. https://doi.org/10.1039/b916757a. Epub 20091209.

42. Gutierrez E, Petrich BG, Shattil SJ, Ginsberg MH, Groisman A, Kasirer-Friede A. Microfluidic devices for studies of shear-dependent platelet adhesion. Lab Chip. 2008;8:9. https://doi.org/10.1039/b804795b. Epub 20080723.

43. Song H, Li HW, Munson MS, Van Ha TG, Ismagilov RF. On-chip titration of an anticoagulant argatroban and determination of the clotting time within whole blood or plasma using a plug-based microfluidic system. Anal Chem. 2006;78(14):4839–49. https://doi.org/10.1021/ac0601718.

44. Middelkamp HHT, Weener HJ, Gensheimer T, Vermeul K, de Heus LE, Albers HJ et al. Embedded macrophages induce intravascular coagulation in 3d blood vessel-on-chip. Biomed Microdevices. 2023;26:1:2. Epub 20231212 https://doi.org/10.1007/s10544-023-00684-w

45. Deng Y, Tay HM, Zhou Y, Fei X, Tang X, Nishikawa M et al. Studying the efficacy of antiplatelet drugs on atherosclerosis by optofluidic imaging on a chip. Lab Chip. 2023;23:3:410–20. Epub 20230131 https://doi.org/10.1039/d2lc00895e

46. Cuartas-Velez C, Middelkamp HHT, van der Meer AD, van den Berg A, Bosschaart N. Tracking the dynamics of thrombus formation in a blood vessel-on-chip with visible-light optical coherence tomography. Biomed Opt Express. 2023;14:11. https://doi.org/10.1364/BOE.500434. Epub 20231009.

47. Zhang Y, Ramasundara SZ, Preketes-Tardiani RE, Cheng V, Lu H, Ju LA. Emerging microfluidic approaches for platelet mechanobiology and interplay with circulatory systems. Front Cardiovasc Med. 2021;8:766513. https://doi.org/10.3389/fcvm.2021.766513. Epub 20211125.

48. Zhang Y, Jiang F, Chen Y, Ju LA. Platelet mechanobiology inspired microdevices: from hematological function tests to disease and drug screening. Front Pharmacol. 2021;12:779753. https://doi.org/10.3389/fphar.2021.779753.

49. Zheng F, Tian R, Lu H, Liang X, Shafiq M, Uchida S, et al. Droplet microfluidics powered hydrogel microparticles for stem cell-mediated biomedical applications. Small. 2024;20:42e2401400. https://doi.org/10.1002/smll.202401400. Epub 20240616.

50. Chow A, Lareau CA. Concepts and new developments in droplet-based single cell multi-omics. Trends Biotechnol. 2024;42:11. https://doi.org/10.1016/j.tibtech.2024.07.006. Epub 20240801.

51. Gantz M, Neun S, Medcalf EJ, van Vliet LD, Hollfelder F. Ultrahigh-throughput enzyme engineering and discovery in in vitro compartments. Chem Rev. 2023;123:9:5571–611. Epub 20230501 https://doi.org/10.1021/acs.chemrev.2c00910

52. Sart S, Ronteix G, Jain S, Amselem G, Baroud CN. Cell culture in microfluidic droplets. Chem Rev. 2022;122:7. https://doi.org/10.1021/acs.chemrev.1c00666. Epub 20220218.

53. Jongen MSA, Holloway PM, Lane SIR, Englyst NA, McCarty OJT, West J. Droplet microfluidics with reagent micromixing for investigating intrinsic platelet functionality. Cell Mol Bioeng. 2021;14:3:223–30. Epub 20210121 https://doi.org/10.1007/s12195-020-00665-6

54. Jongen MSA, MacArthur BD, Englyst NA, West J. Single platelet variability governs population sensitivity and initiates intrinsic heterotypic responses. Commun Biol. 2020;3:1:281. Epub 20200604 https://doi.org/10.1038/s42003-020-1002-5

55. Ganan-Calvo AM, Gordillo JM. Perfectly monodisperse microbubbling by capillary flow focusing. Phys Rev Lett. 2001;87:27. https://doi.org/10.1103/PhysRevLett.87.274501.

Jiang *et al. Journal of Nanobiotechnology*   (2025) 23:171

Page 14 of 14

56. Dreyfus R, Tabeling P, Willaime H. Ordered and disordered patterns in two-phase flows in microchannels. Phys Rev Lett. 2003;90(14):144505. https://doi.org/10.1103/PhysRevLett.90.144505. Epub 20030411.

57. Anna SL, Bontoux N, Stone HA. Formation of dispersions using flow focusing in microchannels. Appl Phys Lett. 2003;82(3):364–6. https://doi.org/10.1063/1.1537519.

58. Ganan-Calvo AM. Generation of steady liquid microthreads and micron-sized monodisperse sprays in gas streams. Phys Rev Lett. 1998;80(2):285–8. https://doi.org/10.1103/PhysRevLett.80.285.

59. Kehe J, Kulesa A, Ortiz A, Ackerman CM, Thakku SG, Sellers D, et al. Massively parallel screening of synthetic microbial communities. Proc Natl Acad Sci U S A. 2019;116:26. https://doi.org/10.1073/pnas.1900102116. Epub 20190611.

60. An O, Deppermann C. Platelet lifespan and mechanisms for clearance. Curr Opin Hematol. 2024;31(1):6–15. Epub 20231030 doi: 10.1097/MOH.0000000000000792.

61. O'Brien JR. Shear-induced platelet aggregation. Lancet. 1990;335:8691:711–3. https://doi.org/10.1016/0140-6736(90)90815-m.

62. Kahner BN, Shankar H, Murugappan S, Prasad GL, Kunapuli SP. Nucleotide receptor signaling in platelets. J Thromb Haemost. 2006;4(11):2317–26. https://doi.org/10.1111/j.1538-7836.2006.02192.x.

63. Jain A, Graveline A, Waterhouse A, Vernet A, Flaumenhaft R, Ingber DE. A shear gradient-activated microfluidic device for automated monitoring of whole blood haemostasis and platelet function. Nat Commun. 2016;7:10176. https://doi.org/10.1038/ncomms10176.

64. Martins Lima A, Bragina ME, Burri O, Bortoli Chapalay J, Costa-Fraga FP, Chambon M, et al. An optimized and validated 384-well plate assay to test platelet function in a high-throughput screening format. Platelets. 2019;30:5563–71. https://doi.org/10.1080/09537104.2018.1514106. Epub 20180905.

65. Chan MV, Armstrong PC, Warner TD. 96-well plate-based aggregometry. Platelets. 2018;29:7. https://doi.org/10.1080/09537104.2018.1445838. Epub 20180315.

66. Polgar J, Matuskova J, Wagner DD. The p-selectin, tissue factor, coagulation triad. J Thromb Haemost. 2005;3:8:1590–6. https://doi.org/10.1111/j.1538-7836.2005.01373.x.

67. Cambien B, Wagner DD. A new role in hemostasis for the adhesion receptor p-selectin. Trends Mol Med. 2004;10:4:179–86 https://doi.org/10.1016/j.molmed.2004.02.007

68. Rubenstein DA, Yin W. Platelet-activation mechanisms and vascular remodeling. Compr Physiol. 2018;8:3. https://doi.org/10.1002/cphy.c170049. Epub 20180618.

69. Ghasemzadeh M, Hosseini E. Platelet-leukocyte crosstalk: linking proinflammatory responses to procoagulant state. Thromb Res. 2013;131:3:191–7. https://doi.org/10.1016/j.thromres.2012.11.028. Epub 20121220.

70. Sperandio M, Smith ML, Forlow SB, Olson TS, Xia L, McEver RP, et al. P-selectin glycoprotein ligand-1 mediates l-selectin-dependent leukocyte rolling in venules. J Exp Med. 2003;197(10):1355–63. https://doi.org/10.1084/jem.20021854.

71. Armstrong PC, Truss NJ, Ali FY, Dhanji AA, Vojnovic I, Zain ZN, et al. Aspirin and the in vitro linear relationship between thromboxane a2-mediated platelet aggregation and platelet production of thromboxane a2. J Thromb Haemost. 2008;6:11. https://doi.org/10.1111/j.1538-7836.2008.03133.x. Epub 20080111.

72. Packham MA, Bryant NL, Guccione MA, Kinlough-Rathbone RL, Mustard JF. Effect of the concentration of ca2 + in the suspending medium on the responses of human and rabbit platelets to aggregating agents. Thromb Haemost. 1989;62:3968–76.

Publisher's note